Joint Propagating Patterns of SST and SLP Anomalies in the North Pacific on Bidecadal and Pentadecadal Timescales

ZHU Yimin (朱益民) and YANG Xiuqun* (杨修群)

Global Ocean-Atmosphere Interaction Laboratory, Department of Atmospheric Sciences,

Nanjing University, Nanjing 210093

ABSTRACT

Wavelet analyses are applied to the Pacific Decadal Oscillation index and North Pacific index for the period 1900–2000, which identifies two dominant interdecadal components, the bidecadal (15–25-yr) and pentadecadal (50–70-yr) modes. Joint propagating patterns of sea surface temperature (SST) and sea level pressure (SLP) anomalies in the North Pacific for the two modes are revealed by using the techniques of multi-channel singular spectrum analysis (MSSA) and linear regression analysis with the global sea surface temperature (GISST) data and the northern hemispheric SLP data for the common period 1903–1998. Significant differences in spatio-temporal structures are found between the two modes. For the bidecadal mode, SST anomalies originating from the Gulf of Alaska appear to slowly spread southwestward, inducing a reversal of early SST anomalies in the central North Pacific. Due to further westward spreading, the SST variation of the central North Pacific leads that of the Kuroshio-Oyashio Extension (KOE) region by approximately 4 to 5 years. Concomitantly, SLP anomalies spread over most parts of the North Pacific during the mature phase and then change into an NPO(North Pacific Oscillation)-like pattern during the transition phase. For the pentadecadal mode, SST anomalies develop in the southeast tropical Pacific and propagate along the North American coast to the mid-latitudes; meanwhile, SST anomalies with the same polarity in the western tropical Pacific expand northward to Kuroshio and its extension region; both merge into the central North Pacific reversing the sign of early SST anomalies there. Accompanying SLP anomalies are characterized by an NPO-like pattern during the mature phase while they are dominant over the North Pacific during the transitional phase. The bidecadal and pentadecadal modes have different propagating patterns, suggesting that the two interdecadal modes may arise from different physical mechanisms.

Key words: Pacific decadal oscillation, interdecadal variation, bidecadal mode, pentadecadal mode

1. Introduction

The climate of the Pacific sector is known to exhibit considerable variability on a wide range of timescales. The strongest interannual fluctuations in the tropical Pacific are primarily associated with the El Niño and Southern Oscillation (ENSO) phenomenon. The mechanism responsible for the existence and evolution of ENSO is relatively well understood. However, the exact nature of the decadal-to-interdecadal climate variability in the Pacific remains unclear and is an area of very active research.

The observational evidence of the decadal-to-interdecadal variability in the Pacific ocean-atmosphere system has attracted more and more at-tention in the past decade. A number of papers have revealed a climatic regime shift around 1976/77 in the North Pacific (Namias et al., 1988; Nitta and Yamada, 1989; Trenberth, 1990; Trenberth and Hurrell, 1994; Graham, 1994; Miller et al., 1994; Zhang and Levitus, 1997; Hare and Mantua, 2000). The results show that for the ocean, the sea surface temperature (SST) tends to be anomalously cool in the central North Pacific and Kuroshio/Oyashio Extension (KOE) but anomalously warm along the North American coast and the central-eastern tropical Pacific; for the atmosphere, the sea level pressure (SLP) and the 500-hPa geopotential height are lower than normal, and the Aleutian low is anomalously strengthened and shifts southeastward. Such a regime shift has a significant impact on

the Pacific and North American climate as well as on the Pacific marine ecosystems.

Spatiotemporal structures of the decadal-to-interdecadal variability over the Pacific have been analyzed with nearly century-long oceanic and atmospheric data records since the late 1990s (Zhang et al., 1997; Mantua et al., 1997; Nakamura et al., 1997). It is found that the climate regime shift in 1976/77 is not unique. Similar regime shifts also occurred in the 1920s and 1940s. Such regime shifts are closely associated with the decadal-to-interdecadal variability in the North Pacific as well as in the tropical Pacific. Mantua et al. (1997) named the variability as the Pacific Decadal Oscillation (PDO), a description of the so-called long-lived ENSO-like mode of the Pacific interdecadal variability revealed by Zhang et al. (1997). The PDO can be clearly distinguished from interannual ENSO variability. Its signature is mostly visible in the North Pacific with a secondary signature existing in the tropics; but the opposite is true for ENSO.

Several studies have found evidence for the direct impact of PDO on the North American climate variability (Latif and Barnett, 1994, 1996; Zhang et al., 1997; Mantua et al., 1997; Mantua and Hare, 2002). Some studies have pointed out possible modulations of PDO to the ENSO-related interannual variability (Wang, 1995; Minobe and Mantua, 1999; Gershunov and Barnett, 1998; Power et al., 1999). The connection between interdecadal variability in the Pacific ocean-atmosphere system and interdecadal climate variation in East Asia and China is also being actively studied (Li, 1998; Li and Li, 2000; Wang, 2001, 2002; Xue, 2001; Zhang and Qian, 2001).

A variety of studies have suggested multiple timescales of the North Pacific decadal-to-interdecadal variability. Latif and Barnett (1994, 1996) analyzed a 125-yr simulation of a coupled ocean-atmosphere model in comparison with observational data, found a coupled mode with a roughly 20-yr period in the North Pacific, and proposed a midlatitude ocean-atmosphere feedback mechanism to explain the mode. Tourre et al. (1999) identified an interdecadal oscillation with a 20–25-yr period using CEOF analysis for the SST, SLP, and upper ocean temperature over the Pacific Ocean and described a full cycle as four different phases. Minobe (1997) first detected a climatic oscillation with a 50–70-yr period in the North Pacific using tree-ring records for the 18th and 19th centuries in the United States and Canada. Minobe (1999, 2000) proposed that the PDO fluctuations were most energetic at periodicities on the bidecadal and pentadecadal timescales, and the climate regime shifts associated with PDO seem to result from the quasi-simultaneous phase reversals of the bidecadal and pentadecadal oscillations. These studies indicate a possibility of the coexistence of multidecadal modes in the North Pacific.

It should be noted, however, that the spatial patterns and their evolutions associated with the multidecadal modes in the North Pacific have not been well documented yet. The issue is addressed in this study by using techniques of the multichannel singular spectral analysis (MSSA) and regression analysis with century-long SST and SLP datasets. The joint propagating patterns of SST and SLP anomalies for two principal interdecadal components, i.e. the bidecadal and pentadecadal modes, are examined. The paper is organized as follows. The data and methodology used in the present analysis are described in section 2. In section 3, a wavelet analysis is applied to the PDO index and the North Pacific index for the period 1900–2000 for determining the dominant timescales of the Pacific interdecadal variability. Sections 4 and 5 depict the joint propagating patterns of the SST and SLP anomalies for the bidecadal mode and the pentadecadal mode, respectively. Significant differences of the propagating patterns between the two modes and possible physical mechanisms are discussed in section 6. The final section is devoted to the conclusion and discussion.

2. Data and methodology

The datasets used in the present work include the PDO index (PDOI) and the NP index (NPI) for the period 1900–2000, the monthly mean sea surface temperature (SST) for the period 1903–1998, and the sea level pressure (SLP) for the period from January 1899 through May 2002. The PDO index is defined as the leading principal component (PC) from an EOF analysis of the monthly SST anomalies poleward of $20°$N in the North Pacific (Zhang et al., 1997; Mantua et al., 1997). The data are provided by Dr. Mantua of Washington University, and are available from the Internet URL: ftp://ftp.atmos.washington.edu/mantua/pnw_impacts/ INDICES/PDO.latest. In parallel with the ENSO phenomenon, extreme phases of the PDO have been classified as being either warm or cool, as defined by SST anomalies in Pacific Ocean. A PDO warm phase (or positive PDOI) is defined when the SST anomaly is negative in the central North Pacific and positive along the North American coast and in the eastern tropical Pacific; the opposite holds true for the PDO cold phase. The NPI is defined as an area-weighted average of the SLP anomaly over the region $30°$N–$65°$N and $160°$E–$140°$W (Trenberth and Hurrell, 1994). The data are available from the Internet URL: http: //www.cgd.ucar.edu/jhurrell/np.html.

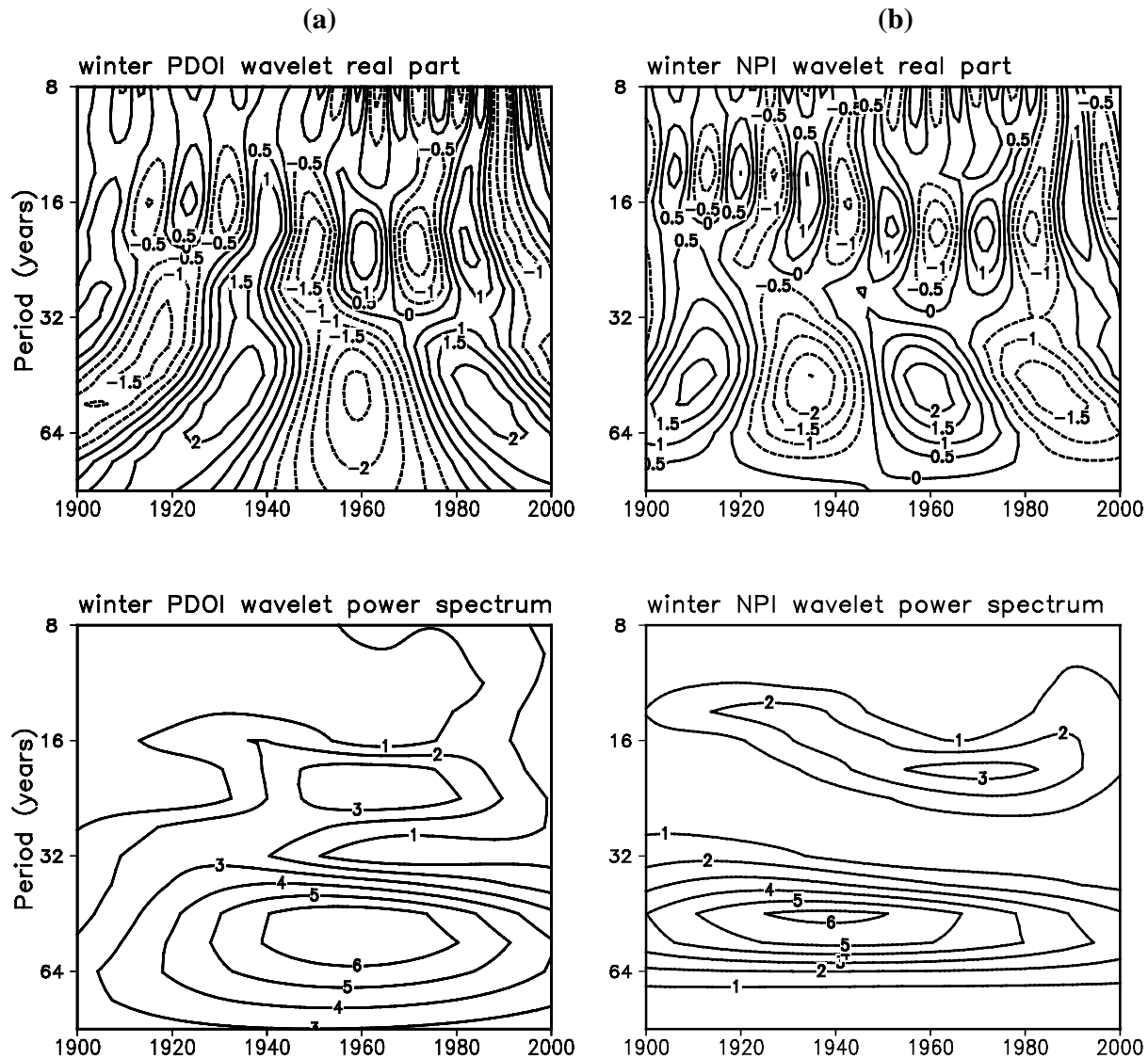**(a)**   **(b)**

Fig. 1. Wavelet coefficients and associated power spectra of (a) the PDOI and (b) the NPI in winter for the period 1900–2000. Contour interval is 0.5 for the wavelet coefficients (upper panel) and 1 for the power spectra (lower panel).

The NPI is highly correlated with the leading PC of the 500-hPa geopotential height anomalies (Trenberth and Hurrell, 1994) as well as the leading PC of the winter SLP anomalies in the North Pacific (Minobe and Mantua, 1999). The NPI and PDOI are two representative indices for the large-scale atmospheric and oceanic variability in the North Pacific. The monthly SST data is taken from the $1° × 1°$ gridded global ice and sea surface temperature (GISST) dataset for the period 1903–1998 (Parker et al., 1995; Rayner et al., 1996). For our research purposes, we select the data over the region from the tropical to extratropical North Pacific (30°S–60°N, 110°E–80°W). The sea

level pressure data is taken from Trenberth's updated version of monthly mean $5°×5°$ gridded northern hemispheric (15°–85°N, 0°–355°E) sea level pressure data from January 1899 through May 2002 (Trenberth and Paolino, 1980). To be consistent with the GISST dataset, we use this SLP data for the common period 1903–1998. Since the SLP data is not readily available in the tropics as well as higher latitudes in the early part of the record, we only analyze the SLP data over the North Pacific region 20°–60°N and 120°E–100°W where the interdecadal variabilities are predominant (Mantua et al., 1997; Mantua and Hare, 2002).

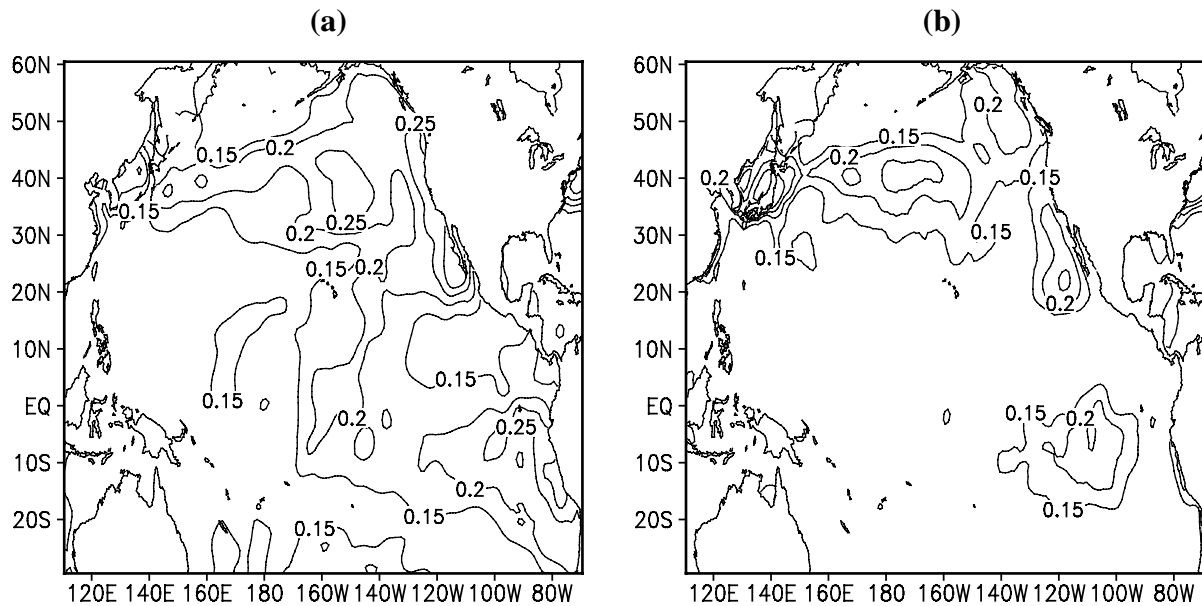First, a Morlet wavelet analysis is applied to the

(a)   **(b)**

Fig. 2. Spatial distributions of the root-mean-square (rms) deviations for the Pacific SST variability on (a) the bidecadal and (b) pentadecadal timescales. Contour interval is 0.05°C.

PDOI and the NPI to examine the dominant timescales of the Pacific variability. The principle of the method and the associated software and user guide are documented in Torrence and Compo (1998). Then, multichannel singular spectrum analysis (MSSA) is used to identify propagating patterns of different interdecadal modes on the dominant timescales. The MSSA method is employed to decompose the decadal-to-interdecadal variability and produce propagating patterns that are optimal in representing variance (Plaut and Vautard 1994). Finally, the linear regression method is used to generate regression maps of coherent evolution of SLP anomalies associated with that of SST anomalies. To focus on the decadal-to-interdecadal timescales, the SST and SLP data are filtered to extract those components with timescales no shorter than 8 years; and the long-term linear trend is removed.

3. Dominant modes of Pacific interdecadal variability

The Morlet wavelet transform was applied to the century-long (1900–2000) winter PDOI and NPI for examining the dominant timescale of interdecadal variability in the Pacific ocean-atmosphere system. Figure 1 displays the wavelet coefficients and associated power spectra in a time-period diagram. It is clearly shown that the wavelet coefficients for either the PDOI (see Fig. 1a) or the NPI (see Fig. 1b) exhibit principal oscillations centered on two distinct time scales roughly with periods 15–25 yr and 50–70 yr. This indicates that the Pacific interdecadal variability is characterized by two dominant modes, a bidecadal mode (15–25 yr) and a pentadecadal mode (50–70 yr). This result qualitatively agrees with the analysis of Minobe (1999, 2000). It can also be seen from Fig. 1 that the periodicity of the bidecadal mode for both indices has experienced a change, an increasing trend, throughout the twentieth century. For the bidecadal mode, shorter periods (roughly 10–15 yr) and weaker amplitudes are observed before the 1940s, whereas longer periods (20–25 yr) and stronger amplitudes are in the mid and late twentieth century. However, no such significant changes occur for the pentadecadal mode.

Another striking feature, as seen from Fig. 1, is the out-of-phase variation of the wavelet coefficients between the PDOI and the NPI on both the bidecadal and pentadecadal timescales. This implies that for either of the decadal timescales, if the central North Pacific is anomalously cool and the North American coast and central-eastern tropical Pacific are anomalously warm (i.e., PDO in its warm phase), then the Aleutian low is anomalously strengthened and moves southeastward, and the opposite occurs in the PDO cold phase. Thus, the coherent feature of the PDOI and the NPI suggests that the Pacific interdecadal variability is attributed to the ocean-atmosphere interaction.
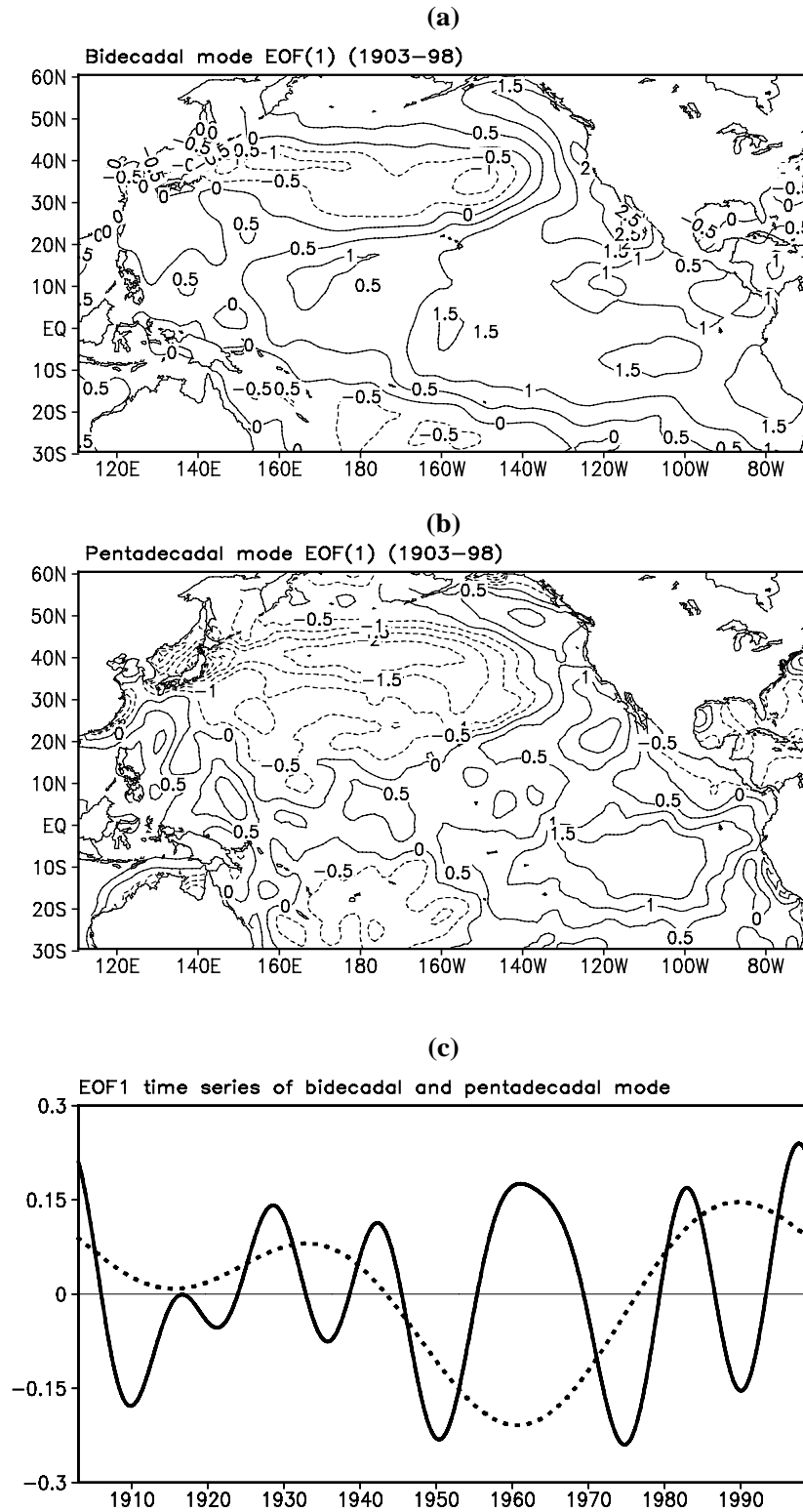
(a)

Bidecadal mode EOF(1) (1903—98)

(b)

Pentadecadal mode EOF(1) (1903—98)

(c)

EOF1 time series of bidecadal and pentadecadal mode

Fig. 3. Leading EOF of SST anomalies on (a) the bidecadal and (b) pentadecadal timescales (Contour interval is 0.5. Solid lines indicate positive values while dashed lines are for negative ones), and (c) their time series (solid line indicates the bidecadal component while dashed line is for the pentadecadal one).

Since the wavelet transform can only depict periodicity or dominant frequency of the interdecadal variability without showing any spatial characteristics, the spatial patterns of the dominant modes for the SST anomaly are identified below for the bidecadal and pentadecadal modes, respectively. The root-mean-square (rms) deviations are calculated using bandpass-filtered SST anomalies for the periods 10–30 yr and 50–70 yr, respectively. As shown in Fig. 2, the spatial distributions of the deviations for the two interdecadal modes look similar. The centers of action for both modes are mainly located in the central North Pacific, KOE region, Gulf of California, and eastern tropical Pacific. However, large deviations are also found in the central tropical Pacific and along the South American coast for the bidecadal mode (see Fig. 2a), which is distinguished from the pentadecadal mode (see Fig. 2b).

To further extract characteristic spatial-temporal structures, EOF analyses are performed for the 10–30 yr and 50–70 yr bandpass-filtered SST anomalies over the Pacific basin. The leading EOFs and associated principal components for the two interdecadal modes are shown in Figs. 3a, b, which account for 44.6% and 52.7% of the total variances, respectively. The EOF for either interdecadal mode is basically characterized by the typical PDO pattern, with the anomaly in the midlatitude North Pacific and the anomaly of opposite polarity in the eastern tropical Pacific and along the North American coast. However, there are some differences between the two modes. The anomalies along the North and South American coasts for the bidecadal mode are more evident than those for the pentadecadal mode. It is quite interesting that there are unique anomalies north of the equator in the western tropical Pacific for the pentadecadal mode, and that such anomalies have a polarity opposite to those in the central North Pacific.

Previous studies have found that the North Pacific experienced three prominent regime shifts respectively in the 1920s, 1940s, and 1970s. Such a feature can be seen from the wavelet analyses of the PDO and NP indices, as shown in Fig. 1. It is striking from the principal components shown in Fig. 3c that the three regime shifts seem to result from quasi-simultaneous phase reversals of the bidecadal and pentadecadal modes with comparable amplitudes. Therefore, superposition and interaction between the bidecadal and pentadecadal modes may play an important role in the Pacific interdecadal variability.

4. Propagating patterns for the bidecadal mode

The wavelet and EOF decomposition analyses described above reveal dominant interdecadal modes and their typical patterns in the North Pacific. Note that the typical pattern examined with EOF frequently re-flects an extreme phase of evolutions for a particular interdecadal mode. For deep understanding of an interdecadal oscillatory mode, it is necessary to discover the spatial features with its full cycling phases including its initiation, development, decay, transition, and recurrence. To get an insight into the evolution or the propagating pattern of SST anomalies for the two interdecadal modes in the North Pacific, a multichannel singular spectrum analysis (MSSA) technique with a given window width is applied to 96 years (1903–1998) of the SST dataset. The window width allows for a reasonable frequency resolution. In terms of the above-mentioned results with wavelet analyses of the PDOI and NPI, 10-yr and 30-yr window widths are thus selected for MSSA to obtain half a cycle evolution of the bidecadal mode and pentadecadal mode, respectively. Meanwhile, to determine coherent evolutions of the bidecadal and pentadecadal modes in SLP anomalies accompanied with those of SST anomalies, a regression method is used in which the SLP anomalies are regressed upon the associated time series of MSSA for SST anomalies.

The joint spatio-temporal evolution of the Pacific bidecadal mode is shown in Fig. 4. The propagating patterns of the bidecadal SST signals obtained by using MSSA with a 10-yr window width are shown in Fig. 4a. The corresponding regressed SLP anomaly patterns over the North Pacific are displayed in Fig. 4b. The bidecadal signals are sampled into five temporal phases representing the evolution of the patterns throughout approximately half a cycle ($\sim$10-yr). The interval of two successive phases is 2 years. The half-cycle evolution can be roughly divided into the following five different stages: mature (Phase 1), decay (Phase 2), transition (Phase 3), development with opposite polarity (Phase 4), and mature with opposite polarity (Phase 5).

During the mature phase, the spatial pattern of SST anomalies is similar to that of the leading EOF in Fig. 3a, showing a typical PDO pattern (Fig. 4a, Phase 1). Assuming that SST anomalies in the central North Pacific are negative, those in the central to eastern tropical Pacific and along the North and South American coasts are accordingly positive. Larger negative SST anomalies occur between $25°$–$45°$N and $170°$E–$150°$W in the central North Pacific. Similar negative SST anomalies also appear in the central South Pacific, but the amplitudes are much weaker. Larger positive SST anomalies appearing near the Gulf of California and Gulf of Alaska are of interest. Another notable feature is that there are few SST anomalies in the western tropical Pacific. For the pan-Pacific basin, the spatial pattern of the bidecadal mode during the mature phase seems to be roughly north-south symmetric about the equator (White and Cayan, 1998; Garreaud and Battisti, 1999). On the other hand, associated with the negative SST anomalies during the mature phase in the central North Pacific, significant negative SLP
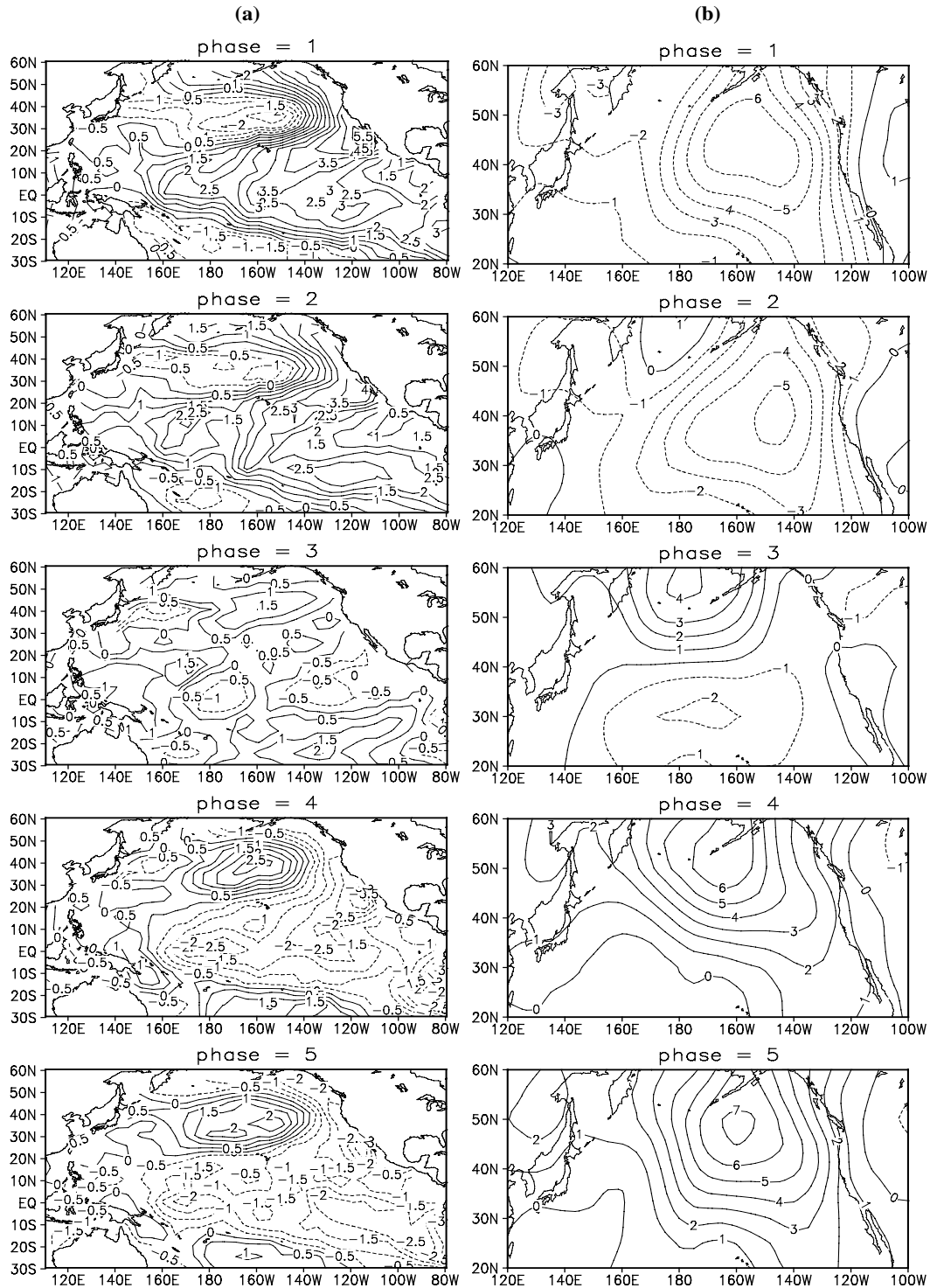
(a)

(b)

Fig. 4. Propagating patterns of (a) SST anomalies and (b) SLP anomalies for the bidecadal mode, as sampled into five successive phases. The interval of two successive phases is 2 years. Note that the patterns for SST are obtained with MSSA technique while those for SLP represent regression coefficients upon the MSSA time series. Contour interval is 0.5 for the SST anomalies and 1 for the SLP anomalies. Solid lines indicate positive values while dashed lines are for negative ones.
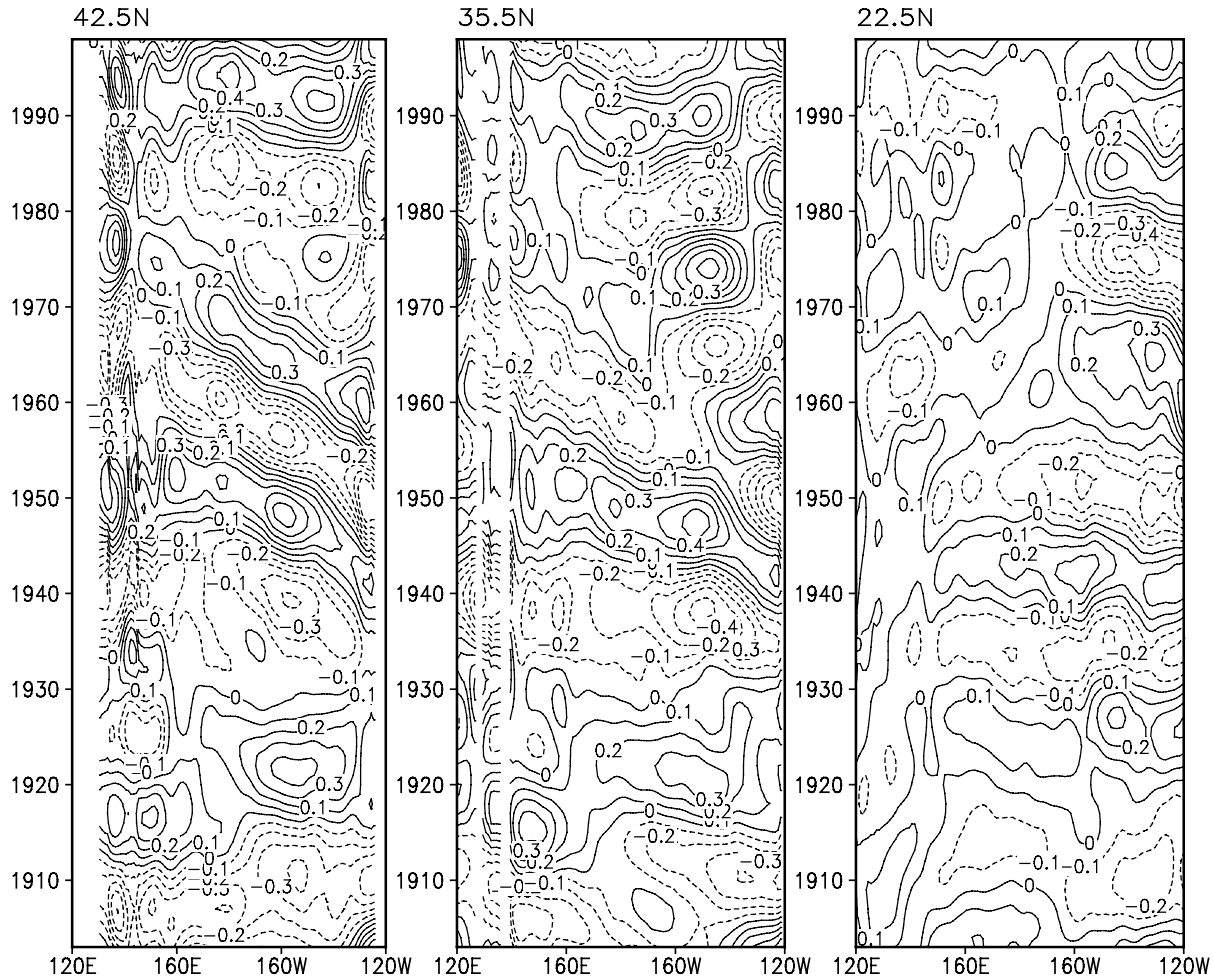
Fig. 5. Time-longitude diagrams of bidecadal SST anomalies along 42.5°N (left panel), 35.5°N (middle panel), and 22.5°N (right panel) during 1903–1998. Contour interval is 0.1°C. Solid lines indicate positive values while dashed lines are for negative ones.

anomalies are spread over most of the North Pacific basin while positive ones cover part of the North American continent (Fig. 4b, Phase 1). The maximal negative SLP anomalies are found between 35°–50°N and 170°–140°W, indicating the strengthening of the Aleutian Low and intensified midlatitude westerlies, which are concurrent with the cooling of the underlying SST in the central to western North Pacific via altering the surface air-sea heat flux exchange, wind mixing, and Ekman advection (Miller et al., 1994). This coherent pattern of SST and SLP anomalies strongly suggests the existence of an ocean-atmosphere interaction inherent in the midlatitude North Pacific. The anomalous zonal gradient of the SLP near the North American coastal region leads to the enhanced southerly anomalies contributing to the warming of the SST in the eastern North Pacific.

During the decay phase, the SST anomalies in the

above-mentioned regions are gradually weakened (Fig. 4a, Phase 2). Accompanied with the weakening of the underlying negative SST anomalies, the negative SLP anomalies also tend to be weakened and slightly shift southward and westward. Meanwhile, the weak positive SLP anomalies occur northwest of the Aleutian Islands and in the western subtropical Pacific (Fig. 4b, Phase 2).

During the transitional phase, the polarity of the SST anomaly signal in the central to eastern tropical Pacific and South American coastal region reverses. Meanwhile, warm SST anomalies originating from the Gulf of Alaska appear to slowly spread southwestward, inducing a reversal of SST anomalies in the central North Pacific. However, cool SST anomalies in the KOE region remain unchanged (Fig. 4a, Phase 3). On the other hand, positive SLP anomalies previously located northwest of the Aleutian Islands are largely

strengthened and move southeastward, indicating a weakening of the Aleutian Low. Previous negative SLP anomalies are obviously weakened and center on the subtropical Pacific region, suggesting a weakening of the subtropical High (Fig. 4b, Phase 3). Therefore, the spatial pattern of the SLP anomalies at this stage is very similar to the so-called North Pacific Oscillation (NPO) pattern, i.e., a seesaw-like oscillation between subtropical High and Aleutian Low (Walker and Bliss, 1932; Rogers, 1981). Consequently, a significant meridional gradient of SLP anomalies is confined along $40°N$ in the North Pacific, resulting in a weakening of the midlatitude westerlies. Concurrent with changes of the SLP anomaly pattern, wind stress curl forcing over the North Pacific is also altered and responsible for the change of underlying SST anomalies via an oceanic Rossby wave which carries SST anomaly signals propagating westward to the central North Pacific and reaching the KOE region several years later.

In the developing phase with opposite polarity, warm SST anomalies in the central North Pacific tend to amplify and gradually migrate westward and reach the KOE region approximately 2–3 years later (Fig. 4a, Phase 4), while positive SLP anomalies continue to enhance and move southeastward (Fig. 4b, Phase 4). Simultaneously, SST anomalies in the central to eastern tropical Pacific and North and South American coasts reverse into cool signals (Fig. 4a, Phase 4). Finally, roughly a decade later, the situation of the entire North Pacific air-sea system completely reverses. Spatial patterns of the SST and SLP anomalies are identical to the initial mature phase but with opposite polarity (see Figs. 4a, b, Phase 5).

An interesting feature identified above with MSSA is the gradual westward migration of SST anomalies from the central North Pacific to the KOE region during the transitional phase. Such a feature can be further confirmed with the 15–25-yr bandpass-filtered SST anomalies along $42.5°N$, $35.5°N$, and $22.5°N$, as shown in Fig. 5. Significant westward propagations are evident along these latitudes, representing the SST anomalies spreading westward from the Gulf of Alaska toward the central and western North Pacific. It should be pointed out, however, that before 1930 this westward propagation is not significant.

Tourre et al. (1999) revealed the evolution of interdecadal SST variability for about 20–25 yr periodicities over the North Pacific basin using CEOF analysis. Their analysis presented a similar result to ours that the SST anomaly signals are found to originate from the Alaskan gyre and move southwestward to the central North Pacific. However, there are still some differences between the two analyses. First, they found another weaker SST anomaly signal with the same polarity originating from the region southeast of Japan ($30°N$, $140°–180°E$) in their analysis. But this signal does not appear in our analysis. Whether this signal is robust enough or not still needs to be further investigated with a longer dataset. Second, in their analysis, during the transition phase, the slow eastward propagation of the relatively weaker SST anomaly signal from the western subtropical gyre and that from the Alaskan gyre merge into the central North Pacific although the eastward propagating signal is much weaker than the one spreading westward. In our analysis, however, the SST anomalies in the central North Pacific first become weaker and then the SST anomalies originating from the Gulf of Alaska gradually propagate westward to the central North Pacific and KOE region inducing a reversal of SST anomalies there. Possible reasons for these discrepancies may be the different data source and time length used in the two studies. SST data used in Tourre et al. (1999) are taken from the Global Ocean Surface Temperature Atlas (GOSTA) and SLP data from the Comprehensive Ocean-Atmosphere Data Set (COADS) for the period 1970–1994, while the present study uses SST data from the GISST dataset and SLP data from Trenberth and Paolino (1980) for the period 1903–1998.

An interesting aspect of our result is that the phase transition of SST anomalies in the central North Pacific and KOE region is not simultaneous. The opposite polarity of SST anomalies appears first in the central North Pacific, and then about 4 to 5 years later, the same transition occurs in the KOE region. That is to say, the SST variation of the central North Pacific leads that of the KOE region by approximately 4 to 5 years (Fig. 4a, Phases 3 to 5). To verify this feature, two area-averaged indices for the 15–25-yr bandpass-filtered SST anomalies are defined over two key regions, the central North Pacific and KOE regions, respectively. Both regions used for the average are selected from Fig. 2a with the rms deviation larger than $0.25°$. Figure 6 exhibits the standardized SST anomaly indices for the central North Pacific (solid line) and the KOE region (dotted line). It is clearly shown that the SST variation of the central North Pacific leads that of the KOE region, which is at least true after 1930. This result is in accordance with the result from MSSA, and also qualitatively consistent with previous analyses (Deser and Blackmon, 1995; Deser et al., 1996; Nakamura et al., 1997; Miller et al., 1998; Miller and Schneider, 2000; Xie, 2000). The reason why it is not true before 1930 is unknown yet. Poor data quality in the early decades of last century might be a candidate cause. Taking the regime shift in 1976/
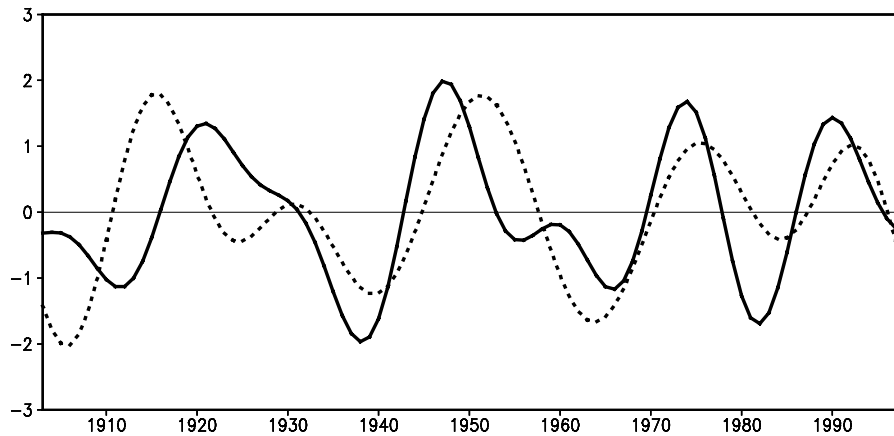
Fig. 6. Standardized time series of area-averaged bidecadal SST anomalies in the central North Pacific (30°–40°N, 165°–145°W; solid line) and the KOE region (35°–40°N, 145°–165°E; dotted line) for the period 1903–1998.

77 for example, the cooling of SST occurred in the central North Pacific, and then approximately five years later, the SST in the KOE region also decreased. This feature has substantial implications to the physical mechanism responsible for the bidecadal mode. It is noteworthy that Latif and Barnett (1994, 1996) proposed a midlatitude ocean-atmosphere feedback mechanism to explain a coupled ocean-atmosphere model that exhibits oscillations with a roughly 20-yr period. According to their hypothesis, the reversal of negative SST anomalies in the central Pacific should be attributed to the warm water transfer of Kuroshio as a branch of the subtropical gyre, and thus the SST anomalies in the KOE region should lead those in the central Pacific. Obviously, there are inconsistencies between observational facts and the hypothesis of Latif and Barnett (1994, 1996).

5. Propagating patterns for the pentadecadal mode

Figure 7 exhibits the joint spatio-temporal evolution of the pentadecadal mode for SST and SLP anomalies. Propagating patterns of the pentadecadal SST signals are computed by using the MSSA technique with a 30-yr window width, as shown in Fig. 7a. The corresponding regressed SLP anomaly patterns upon the MSSA time series are displayed in Fig. 7b. The pentadecadal signals are sampled into eight temporal phases representing the evolution of those patterns throughout approximately half a cycle (∼32-yr). The interval of two successive phases is 4 years. Similar to the analysis for the bidecadal mode, the half-cycle evolution for the pentadecadal mode can also be roughly divided into the following five different stages:

mature (Phases 1 and 2), decay (Phases 3 to 5), transition (Phase 6), development with opposite polarity (Phase 7), and mature with opposite polarity (Phase 8).

During the mature phase, the spatial pattern of the pentadecadal mode is marked by the SST anomalies in the central and western North Pacific changing inversely with those in the tropical central and southeast Pacific (Fig. 7a, Phases 1 to 2). When warm SST anomalies occur in the central and eastern tropical Pacific, cool SST anomalies appear in the central and western North Pacific and the central South Pacific. The maximal cool SST anomaly region in the central North Pacific is confined in 35°–45°N and 160°E–150°W. Cool SST anomalies in the central South Pacific are much weaker. Significant warm SST anomalies are found over the region 0°–15°S and 130°–90°W in the central and eastern Pacific. Correspondingly, SLP anomalies are characterized by an NPO-like pattern, negative SLP anomalies centered on the Aleutian Islands, and positive SLP anomalies in the subtropical Pacific (Fig. 7b, Phases 1 to 2). This pattern persists throughout the early period of the half cycle.

During the decay phase, SST anomalies appear to alter significantly (Fig. 7a, Phases 3 to 5). Warm SST anomalies in the central tropical Pacific weaken quickly so that major warm SST anomalies are limited in the eastern tropical Pacific. Meanwhile, warm SST anomaly signals appear in the Gulf of Alaska that can partially be traced back to those in the tropical eastern Pacific. It is obviously shown that warm SST anomalies in the eastern tropical Pacific extend gradually along the North American coast to the midlatitudes and merge into the weaker anomalies of the same polarity in the Gulf of Alaska roughly after 4–5 years.
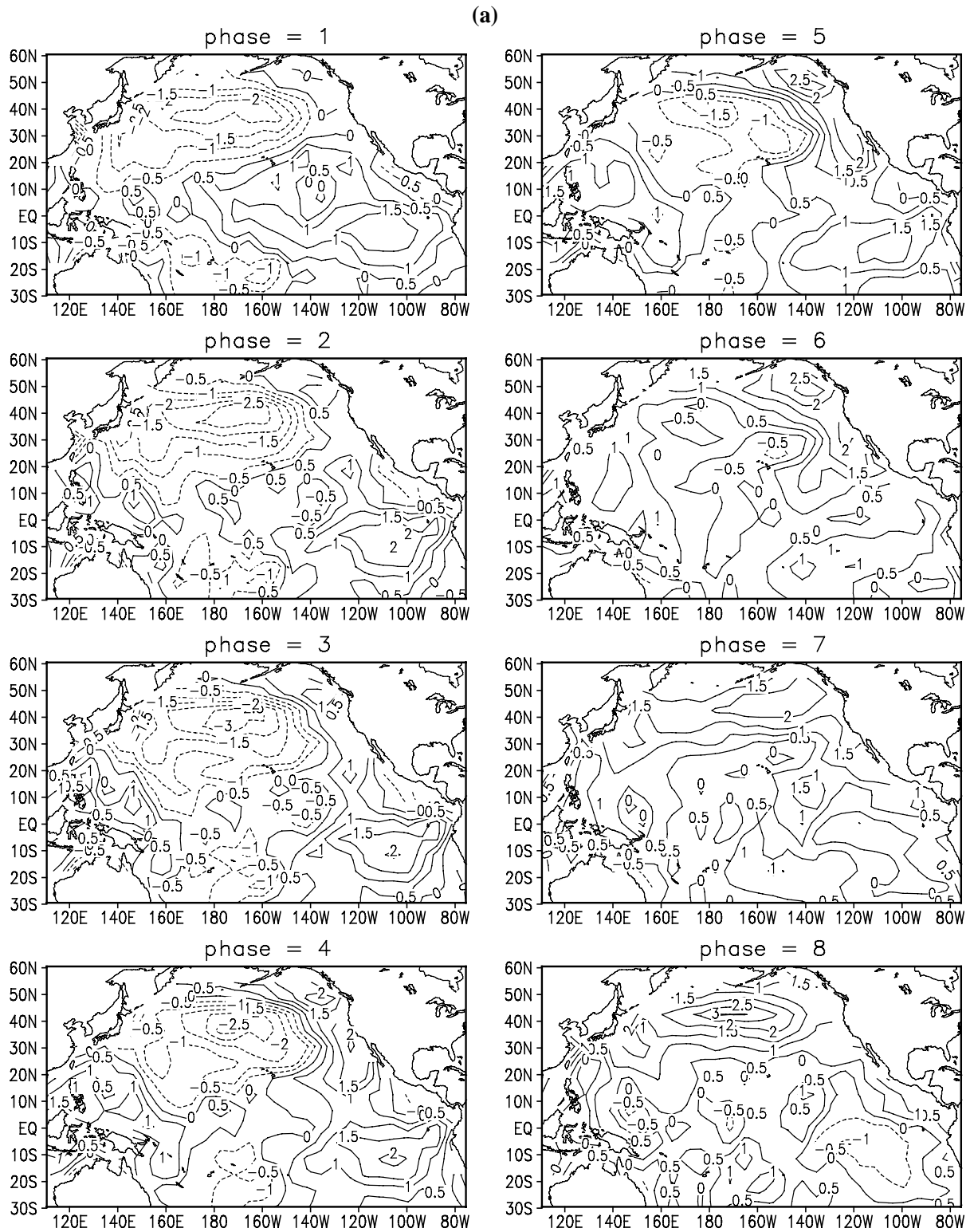
(a)

Fig. 7. Propagating patterns of (a) SST anomalies and (b) SLP anomalies for the pentadecadal mode, as sampled into eight successive phases. The interval of two successive phases is 4 years. All others are the same as in Fig. 4.
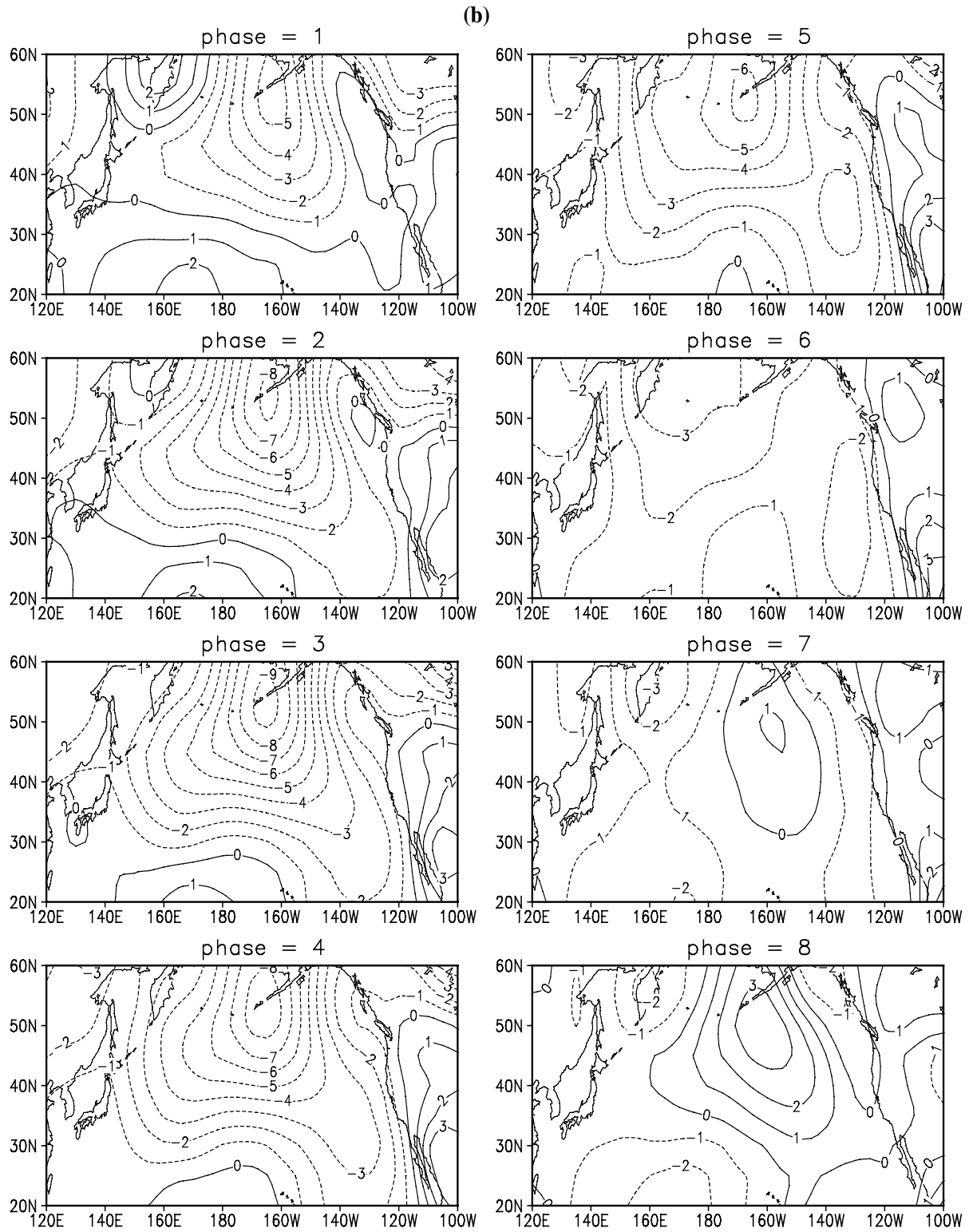
(b)

Fig. 7. (Continued)

Thus, the whole region along the North American coast appears to be warm (Fig. 7a, Phase 5). Besides the above northward migration of SST anomalies along Californian coast, another striking feature is that the similar phenomenon takes place in the western Pacific. While warm SST anomalies decay in the central tropical Pacific, they develop in the tropical western Pacific. Importantly, these warm SST anomalies expand northward to Kuroshio and its extension region but lag those in the eastern tropical Pacific by approximately 12–16 years. In correspondence with the above SST anomalies, negative SLP anomalies keep growing and expend toward the eastern subtropical Pacific, reversing the sign of SLP anomalies near the western coast of North America. Meanwhile, concurrent with the propagation of warm SST anomalies along the coast, positive SLP anomalies also develop northward in the western North America continent, indicating an enhancement of the zonal SLP gradient across the coast (Fig. 7b, Phases 3 to 5). The resultant anomalous southerly likely induces a weakening of the coastal upwelling that may contribute to maintain warm SST anomalies along the coast. At the same time, positive SLP anomalies over the western subtropical Pacific gradually weaken.

During the transitional phase, SST anomalies in the Gulf of Alaska that originate from the eastern tropical Pacific expand westward, while those in the KOE region expand eastward. Both converge into the central North Pacific poleward of 35°N, reversing the sign of the early SST anomalies there (Fig. 7a, Phases 6–8). Positive SLP anomalies emerge in the vicinity of the Aleutian region, replacing the original negative ones (Fig. 7b, Phase 7). The early positive SLP anomalies in the subtropical region disappear and then reverse into negative ones. Thus, the NPO-like pattern finally changes from its positive phase into the negative one. A similar transition also occurs in the North American continent (Fig. 7b, Phases 6–8). Consequently, the spatial pattern is entirely reversed and the evolution during a half cycle for the pentadecadal mode is completed.

To further confirm above evolutional processes, temporal variations of the 50–70-yr bandpass-filtered SST anomalies along 42.5°N, 35.5°N, and 22.5°N are shown in Fig. 8. A significant westward propagation feature is clearly seen along 42.5°N and 35.5°N (Fig. 8, left and middle panel), which depicts the migration of SST anomalies along the North American coast from the eastern tropical Pacific to the midlatitudes and their westward spreading from the Gulf of Alaska to the central North Pacific. Meanwhile, a significant eastward propagation feature is observed along 22.5°N (Fig. 8, right panel), which indicates that the SST

anomalies in the tropical western Pacific spread northeastward and finally merge in the central North Pacific with those SST anomalies coming from the eastern boundary.

6. Differences between the two modes and possible mechanism

The previous sections provide a detailed description of joint propagating patterns for SST and SLP anomalies for the bidecadal and pentadecadal modes, which indicates that such modes possess different spatio-temporal structures and evolutional processes.

As for the spatial structure, the SST anomaly pattern for the bidecadal mode is characterized by a north-south symmetry about the equator, similar to a typical PDO pattern revealed by Mantua et al. (1997), while prominent SLP anomalies centered on the southeast Aleutian Islands spread all over most parts of the North Pacific. For the pentadecadal mode, SST anomalies in the central and western North Pacific are opposite to those in the tropical central and southeast Pacific; the associated SLP anomalies are mainly characterized by an NPO-like pattern, i.e., a seesaw-like change of SLP between the subpolar and subtropical regions.

As for the evolutionary process, the two modes also show significant differences. For the bidecadal mode, typical features are that SST anomalies originating from the Gulf of Alaska appear to slowly spread southwestward, inducing a reversal of early SST anomalies in the central North Pacific, and that the SST variation in the central North Pacific leads that in the KOE region by approximately 4–5 years. Corresponding to the matured SST anomalies in the central North Pacific, SLP anomalies with the same polarity appear to dominate all over the North Pacific. During the transitional phase of the bidecadal SST mode, the SLP anomalies change into an NPO-like pattern, although it exists for a relatively short period.

For the pentadecadal mode, the SST anomalies in the southeast tropical Pacific appear to propagate along the North America coast to the midlatitudes, accompanied by a northward growth of SLP anomalies over western North America. Meanwhile, the SST anomalies in the western tropical Pacific also expand northward to Kuroshio and its extension. Both merge into the central North Pacific reversing the sign of early SST anomalies there. In contrast to the bidecadal mode, the matured pentadecadal SST mode coincides with an NPO-like SLP pattern, while during its transitional phase the SLP anomalies are dominant all over the North Pacific. This indicates that although both of the modes exhibit similar NPO-like patterns,
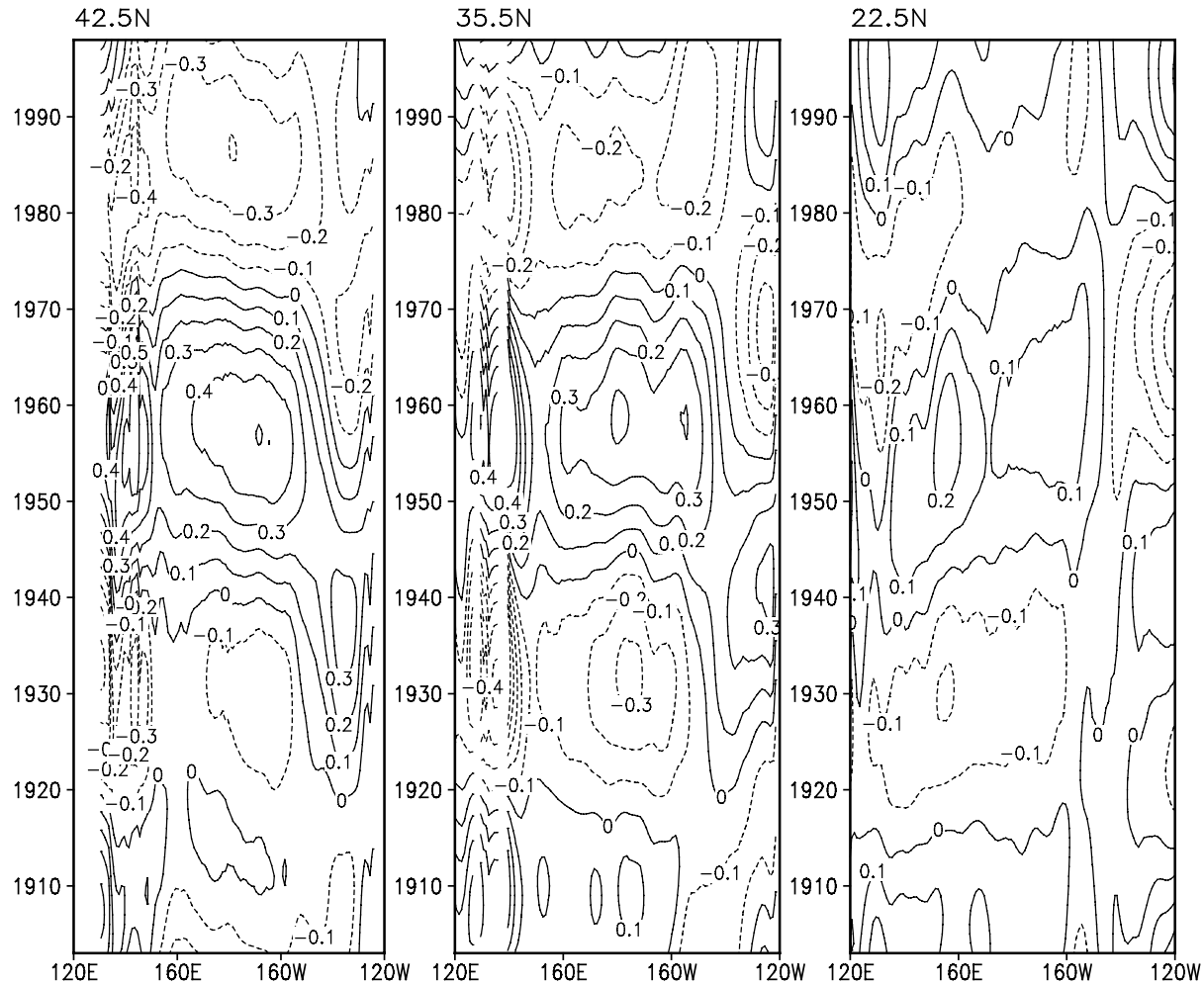
Fig. 8. The same as in Fig. 5, except for the pentadecadal SST anomalies.

this happens in the transition phase with a shorter duration for the bidecadal mode, but in the mature phase with a longer duration for the pentadecadal mode.

These significant differences between the bidecadal and pentadecadal modes suggest that the two interdecadal modes likely arise from different physical mechanisms. The present work provides some implications on their possible mechanisms. The candidate mechanism responsible for the bidecadal mode may be considered as follows. The SLP anomalies characterized by an anomalous change of the intensity of the Aleutian Low and midlatitude westerlies directly force the underlying SST anomalies in the central North Pacific via Ekman advection, vertical mixing, and air-sea heat exchange. Meanwhile, the SLP anomalies also cause the change of wind stress curl as well as the associated Ekman pumping, inducing westward-propagating oceanic Rossby waves. After several years, these Rossby waves arrive at the western boundary and lead to the adjustment of subtropical

and subpolar gyres and their western boundary currents. Thus, the SST anomalies in the KOE region, which are of the same polarity as those in the central North Pacific, might be a lag response to the previous change of wind stress curl in the central North Pacific. The possible mechanism of the bidecadal mode may involve the delayed negative feedback associated with the local adjustments of the North Pacific gyres.

Interaction between the tropical Pacific and midlatitude North Pacific may play an important role in the pentadecadal mode. Some researchers have indicated that the northward-propagating oceanic Kelvin wave along the eastern boundary of the Pacific basin can communicate information between the tropics and midlatitudes. Such a wave can radiate baroclinic Rossby waves in the midlatitudes, which can exert an influence on the central North Pacific (Jacobs et al., 1994; Miller et al., 1997; Meyers et al., 1996; Clarke and Lebedev, 1999). Our analysis in the present study supports the mechanism. Besides this mechanism, the

present analysis also indicates that Kuroshio transfer in the western North Pacific can jointly play an important role in reversing SST anomalies in the central North Pacific. Thus, the possible mechanism for the pentadecadal mode may involve a kind of long-distance delayed negative feedback, which could be related to the tropics-extratropics interaction.

In order to understand and predict future interdecadal climate variations, it is very important to understand their physical mechanisms, although so far they remain unclear. Several hypotheses have been made on the mechanism for the bidecadal mode, however there are still many uncertainties and even contradictions (Miller and Schneider, 2000). As for the pentadecadal mode, however, no hypothesis has been proposed yet. In the present work, we tentatively discuss the possible physical mechanism for the bidecadal and pentadecadal modes based on the diagnostic analysis of observational SST and SLP data. However, all these speculations should be further investigated with the coupled ocean-atmosphere models. More quantitative analyses and numerical simulations could shed more light on this issue.

7. Summary and concluding remarks

This study investigates dominant timescales of the interdecadal variability in the Pacific ocean-atmosphere system. Wavelet analyses are applied to two kinds of climatic indices, PDOI and NPI, which identifies two dominant interdecadal modes, i.e., the bidecadal (15–25-yr) mode and the pentadecadal (50–70-yr) mode. Spatiotemporal structures of the SST anomalies in the North Pacific for the two interdecadal modes are revealed using a MSSA technique. The SST data are taken from the GISST dataset for the period 1903–1998. The covarying SLP anomalies are reconstructed by using linear regression method based on the associated time coefficients of MSSA. Joint propagating patterns of SST and SLP anomalies in the North Pacific for the bidecadal and pentadecadal modes are documented.

Analyses show significant differences in the propagating patterns between the two modes. The bidecadal SST mode possesses a typical PDO pattern with a spatial structure roughly symmetric about the equator. For such a mode, the SST anomalies originating from the Gulf of Alaska appear to slowly spread southwestward, therefore inducing a reversal of early SST anomalies in the central North Pacific. Due to further westward spreading, the SST variation of the central North Pacific leads that of the KOE region by approximately 4–5 years. In accordance with the propagating

patterns of SST anomalies, prominent SLP anomalies centered on the southeast Aleutian Islands spread all over most parts of the North Pacific during the mature phase of the bidecadal mode, and then they move southward and westward until another SLP signal with opposite polarity develops in high latitudes, thus consisting of an NPO-like pattern during the transitional phase.

For the pentadecadal mode, SST anomalies in the central and western North Pacific are opposite to those in the tropical central and southeast Pacific; the associated SLP anomalies are mainly characterized by an NPO-like pattern, i.e., a seesaw-like change of SLP between the subpolar and subtropical regions. The SST anomalies in the southeast tropical Pacific appear to propagate along the North American coast to the midlatitudes, accompanied by a northward growth of SLP anomalies over western North America. Meanwhile, the SST anomalies in the western tropical Pacific also expand northward to Kuroshio and its extension. Both merge into the central North Pacific reversing the sign of early SST anomalies there. In contrast to the bidecadal mode, the matured pentadecadal SST mode coincides with an NPO-like SLP pattern, while during its transitional phase the SLP anomalies are dominant all over the North Pacific. This indicates that although both of the modes exhibit similar NPO-like patterns, it happens during the transitional phase for the bidecadal mode but during the mature phase for the pentadecadal mode.

Consequently, the bidecadal and pentadecadal modes have different spatiotemporal structures and evolutionary processes, suggesting that the two interdecadal modes may arise from different physical mechanisms. For the bidecadal mode, SST anomalies in the central North Pacific might be a direct response to the overlying atmospheric forcing by Ekman advection, vertical mixing, and air-sea heat exchange associated with the SLP anomaly pattern. But the lagged SST anomalies in the KOE region with the same polarity as those in the central North Pacific are caused by the westward propagation of oceanic Rossby waves excited by the previous wind stress curl anomalies over the central North Pacific. For the pentadecadal mode, the northward propagation of SST anomalies from the tropics to midlatitudes at both the eastern and western boundaries suggests that the interaction between the tropical Pacific and the midlatitude North Pacific may play a crucial role. The interaction could be attributed not only to the northward-propagating Kelvin wave at the eastern boundary, but also to the Kuroshio transfer at the western boundary. Thus, possible mechanisms for the bidecadal mode may involve a

delayed negative feedback associated with local adjustments of North Pacific gyres, while those for the pentadecadal mode may involve a long-distance delayed negative feedback associated with oceanic anomalies propagating between the tropics and extratropics.

REFERENCES

Clarke, A. J., and A. Lebedev, 1999: Remotely driven decadal and longer changes in the coastal Pacific waters of the Americas. *J. Phys. Oceanogr.*, **29**, 828–835.

Deser, C., and M. L. Blackmon, 1995: On the relationship between tropical and North Pacific sea surface temperature variations. *J. Climate*, **8**, 1677–1680.

Deser, C., M. A. Alexander, and M. S. Timlin, 1996: Upper ocean thermal variations in the North Pacific during 1970–1991. *J. Climate*, **9**, 1840–1855.

Garreaud, R. D., and D. S. Battisti, 1999: Interannual (ENSO) and interdecadal (ENSO-like) variability in the Southern Hemisphere tropospheric circulation. *J. Climate*, **12**, 2113–2122.

Gershunov, A., and T. P. Barnett, 1998: Interdecadal modulation of ENSO teleconnection. *Bull. Amer. Meteor. Soc.*, **79**, 2715–2725.

Graham, N. E., 1994: Decadal scale variability in the 1970s and 1980s: Observations and model results. *Climate Dyn.*, **10**, 135–162.

Hare, S. R., and N. J. Mantua, 2000: Empirical evidence for North Pacific regime shifts in 1977 and 1989. *Progress in Oceanography*, **47**, 103–145.

Jacobs, G. A., H. E. Hurlburt, J. C. Kindle, E. J. Metzger, J. L. Mitchell, W. J. Teague, and A. J. Wallcraft, 1994: Decade-scale trans-Pacific propagation and warming effects of an El Niño anomaly. *Nature,* **370**, 360–363.

Latif, M., and T. P. Barnett, 1994: Causes of decadal climate variability over the North Pacific and North America. *Science*, **266**, 634–637.

Latif, M., and T. P. Barnett, 1996: Decadal climate variability over the North Pacific and North America: Dynamics and predictability. *J. Climate*, **9**, 2407–2423.

Li Chongyin, 1998: The quasi-decadal oscillation of air-sea system in the Northwestern Pacific region. *Advances in Atmospheric Sciences*, **15**(1), 31–40.

Li Chongyin, and Li Guilong, 2000: The NPO/NAO and interdecadal climate variation in China. *Advances in Atmospheric Sciences*, **17**(4), 555–561.

Mantua, N. J., S. R. Hare, Y. Zhang, J. M. Wallace, and R. C. Francis, 1997: A Pacific interdecadal climate oscillation with impacts on salmon production. *Bull. Amer. Meteor. Soc.*, **78**, 1069–1079.

Mantua, N. J. and S. R. Hare, 2002: The Pacific Decadal Oscillation. *J. Oceanogr.*, **58**, 35–44.

Meyers, S. D., M. A. Johnson, M. Liu, J. J. O'Brien, and J. L. Spiesberger, 1996: Interdecadal variability in a numerical model of the northeast Pacific Ocean: 1970–89. *J. Phys. Oceanogr.*, **26**, 2635–2652.

Miller, A. J., D. R. Cayan, T. P. Barnett, N. E. Graham, and J. M. Oberhuber, 1994: The 1976–1977 climate shift of the Pacific Ocean. *Oceanography*, **7**, 21–26.

Miller, A. J., W. B. White, and D. R. Cayan, 1997: North Pacific thermocline variations on ENSO timescales. *J. Phys. Oceanogr.*, **27**, 2023–2039.

Miller, A. J., Cayan, D. R., and W. B. White, 1998: A westward intensified decadal change in the North Pacific thermocline and gyre-scale circulation. *J. Climate*, **11**, 3112–3127.

Miller, A. J. and N. Schneider, 2000: Interdecadal climate regime dynamics in the North Pacific Ocean: Theories, observations and ecosystem impacts. *Progress in Oceanography*, **47**, 355–379.

Minobe, S., 1997: A 5070 year climatic oscillation over the North Pacific and North America. *Geophys. Res. Lett.*, **24**, 683–686.

Minobe, S., and N. J. Mantua, 1999: Interdecadal modulation of interannual atmospheric and oceanic variability over the North Pacific. *Progress in Oceanography*, **43**, 163–192.

Minobe, S., 1999: Resonance in bidecadal and pentadecadal climate oscillations over the North Pacific: Role in climatic regime shifts. *Geophys. Res. Lett.*, **26**, 855–858.

Minobe, S., 2000: Spatiotemporal structure of the pentadecadal variability over the North Pacific. *Progress in Oceanography*, **47**, 381–408.

Nakamura, H., G. Lin, and T. Yamagata, 1997: Decadal climate variability in the North Pacific during the recent decades. *Bull. Amer. Meteor. Soc.*, **98**, 2215–2225.

Namias, J., X. Yuan, and D. R. Cayan, 1988: Persistence of North Pacific sea surface temperature and atmospheric flow patterns. *J. Climate*, **1**, 682–703.

Nitta, T., and S. Yamada, 1989: Recent warming of tropical sea surface temperature and its relationship to the Northern Hemisphere circulation. *J. Meteor. Soc. Japan*, **67**, 375–383.

Parker, D. E., C. K. Folland, and M. Jackson, 1995: Marine surface temperature: Observed variations and data requirements. *Climate Change*, **31**, 559–600.

Plaut, G. and R. Vautard, 1994: Spells of low-frequency oscillation and weather regimes in the Northern Hemisphere. *J. Atmos. Sci.*, **51**, 210–236.

Power, S., T. Casey, C. Folland, A. Colman, and V. Mehta, 1999: Interdecadal modulation of the impact of ENSO on Australia. *Climate Dyn.*, **15**, 319–324.

Rogers, J. C., 1981: The North Pacific Oscillation. *J. Climatol.*, **1**, 39–57.

Rayner, N. A., E. B. Horton, D. E. Parker, C. K. Folland, and R. B. Hackett, 1996: Version 2.2 of the global sea-ice and sea surface temperature data set, 1903-1994. *Clim. Res. Tech. Note*, **74**, 1–21.

Torrence, C., and G. P. Compo, 1998: A practical guide to wavelet analysis. *Bull. Amer. Meteor. Soc.* **79**, 61–78.

Trenberth, K. E., and D. A. Paolino, 1980: The Northern Hemisphere sea-level pressure data set: Trends, errors, and discontinuities. *Mon. Wea. Rev.*, **108**, 855–872.

Trenberth, K. E., 1990: Recent observed interdecadal climate changes in the Northern Hemisphere. *Bull. Amer. Meteor. Soc.*, **71**, 988–993.

Trenberth, K. E., and J. W. Hurrell, 1994: Decadal atmosphereocean variations in the Pacific. *Climate Dyn.*, **9**, 303–319.

Tourre, Y., W. B. White, and Y. Kushnir, 1999: Evolution of interdecadal variability in sea level pressure, sea surface temperature, and upper ocean temperature over the Pacific Ocean. *J. Phys. Oceanogr.*, **29**, 1528–1541.

Walker, G. T., and E. W. Bliss, 1932: World weather. *Mem. Roy. Meteor. Soc.*, **4**, 29–64.

Wang, B., 1995: Interdecadal changes in El Niño onset in the last four decades. *J. Climate*, **8**, 267–285.

Wang Huijun, 2001: The weakening of the Asian Monsoon Circulation after the end of 1970's. *Advances in Atmospheric Sciences*, **18(3)**, 374–386.

Wang Huijun, 2002: The instability of the East Asian Summer Monsoon-ENSO relations. *Advances in Atmospheric Sciences*, **19**(1), 1–11.

White, W. B., and D. R. Cayan., 1998: Quasi-periodicity and global symmetries in interdecadal upper ocean temperature variability. *J. Geophys. Res.*, **103**, 21335–21354.

Xie, S. P., 2000: Interdecadal thermocline variability in the North Pacific for 1958-97: A GCM simulation. *J. Phys. Oceanogr.*, **30**, 2798–2813.

Xue Feng, 2001: Interannual to interdecadal variation of East Asian Summer Monsoon and its association with the global atmospheric circulation and sea surface temperature. *Advances in Atmospheric Sciences*, **18**(4), 567–575.

Zhang, R. H., and S. Levitus, 1997: Structure and cycle of decadal variability of upper-ocean temperature in the North Pacific. *J. Climate*, **10**, 710–727.

Zhang Weiqing and Qian Yongfu, 2001: The relationships between variations of sea surface temperature anomalies in the key ocean areas and the precipitation and surface air temperature in China. *Advances in Atmospheric Sciences*, **18**(2), 294–308.

Zhang, Y., J. M. Wallace, and D. S. Battisti, 1997: ENSO-like interdecadal variability: 1900–93. *J. Climate*, **10**, 1004–1020.